

Title	Mice expressing aberrant sperm-specific protein PMIS2 produce normal-looking but fertilization-incompetent spermatozoa
Author(s)	Yamaguchi, Ryo; Fujihara, Yoshitaka; Ikawa, Masahito et al.
Citation	Molecular Biology of the Cell. 23(14) p.2671-p.2679
Issue Date	2012-07-15
oaire:version	VoR
URL	https://hdl.handle.net/11094/78610
rights	© 2012 Yamaguchi et al. This article is licensed under a Creative Commons Attribution-NonCommercial-ShareAlike 3.0 Unported License.
Note	

Osaka University Knowledge Archive : OUKA

<https://ir.library.osaka-u.ac.jp/>

Osaka University

Mice expressing aberrant sperm-specific protein PMIS2 produce normal-looking but fertilization-incompetent spermatozoa

Ryo Yamaguchi^{a,b}, Yoshitaka Fujihara^a, Masahito Ikawa^a, and Masaru Okabe^{a,b}

^aResearch Institute for Microbial Diseases and ^bGraduate School of Pharmaceutical Sciences, Osaka University, Suita, Osaka 565-0871, Japan

ABSTRACT Eight kinds of gene-disrupted mice (*Clgn*, *Calr3*, *Pdilt*, *Tpst2*, *Ace*, *Adam1a*, *Adam2*, and *Adam3*) show impaired sperm transition into the oviducts and defective sperm binding to the zona pellucida. All of these knockout strains are reported to lack or show aberrant expression of a disintegrin and metallopeptidase domain 3 (ADAM3) on the sperm membrane. We performed proteomic analyses of the proteins of these infertile spermatozoa to clarify whether the abnormal function is caused exclusively by a deficiency in ADAM3 expression. Two proteins, named PMIS1 and PMIS2, were missing in spermatozoa from *Clgn*-disrupted mice. To study their roles, we generated two gene-disrupted mouse lines. *Pmis1*-knockout mice were fertile, but *Pmis2*-knockout males were sterile because of a failure of sperm transport into the oviducts. *Pmis2*-deficient spermatozoa also failed to bind to the zona pellucida. However, they showed normal fertilizing ability when eggs surrounded with cumulus cells were used for in vitro fertilization. Further analysis revealed that these spermatozoa lacked the ADAM3 protein, but the amount of PMIS2 was also severely reduced in *Adam3*-deficient spermatozoa. These results suggest that PMIS2 might function both as the ultimate factor regulating sperm transport into the oviducts and in modulating sperm–zona binding.

Monitoring Editor

Julie Brill
The Hospital for Sick Children

Received: Dec 19, 2011

Revised: May 16, 2012

Accepted: May 16, 2012

INTRODUCTION

The mammalian fertilization process starts with the deposition of spermatozoa into the female reproductive tract (in the mouse, directly into the uterus, and in the human, into the vagina). The spermatozoa are then required to migrate to the oviduct, where the ovulated eggs and spermatozoa meet (Suarez, 2008). Gene disruption experiments have been used to produce at least eight lines of specific gene-disrupted mouse lines with knockouts for *Clgn* (Ikawa

et al., 1997), *Calr3* (Ikawa et al., 2011), *Pdilt* (Tokuhiro et al., 2012), *Tpst2* (Marcello et al., 2011), *Ace* (Krege et al., 1995), *Adam1a* (Nishimura et al., 2004), *Adam2* (Cho et al., 1998), and *Adam3* (Shamsadin et al., 1999). In these mice, the spermatozoa show impaired migration into the oviduct, whereas their motility remains unaffected. The spermatozoa from all of these gene-knockout (KO) mouse lines were shown to have lost their zona-binding ability when mixed with cumulus-free eggs in vitro. The mechanisms were not clarified, but as reported for *Adam1a*, *Adam3*, and *Pdilt* KO lines (Nishimura et al., 2004; Tokuhiro et al., 2012), these mutant spermatozoa could fertilize cumulus-surrounded eggs. This indicates that the primary cause for infertility in these mouse strains is not a defect in sperm–zona binding but the inability of spermatozoa to migrate from the uterus into the oviduct.

Zamboni (1972) reported that in the mouse the uterotubal junction (UTJ) is patent for only a short time after mating. However, as just indicated, spermatozoa from various gene-disrupted mouse strains failed to migrate into the oviducts at the normal time. This indicates that UTJ patency is not controlled solely by the female's physiology after mating. If the UTJ barrier opens in response to

This article was published online ahead of print in MBoc in Press (<http://www.molbiolcell.org/cgi/doi/10.1091/mboc.E11-12-1025>) on May 23, 2012.

Address correspondence to: Masaru Okabe (okabe@biken.osaka-u.ac.jp).

Abbreviations used: DTT, dithiothreitol; eCG, equine chorionic gonadotropin; EST, expressed sequence tag; GFP, green fluorescent protein; hCG, human chorionic gonadotropin; IVF, in vitro fertilization; LC-MS/MS, liquid chromatography tandem mass spectrometry; RT-PCR, reverse transcription PCR; UTJ, uterotubal junction.

© 2012 Yamaguchi et al. This article is distributed by The American Society for Cell Biology under license from the author(s). Two months after publication it is available to the public under an Attribution–Noncommercial–Share Alike 3.0 Unported Creative Commons License (<http://creativecommons.org/licenses/by-nc-sa/3.0>).

"ASCB®," "The American Society for Cell Biology®," and "Molecular Biology of the Cell®" are registered trademarks of The American Society of Cell Biology.

wild-type (WT) spermatozoa or to some male factors, those spermatozoa that cannot pass through the UTJ might have their transport “rescued” with the coexistence of WT spermatozoa. Previously, we examined this possibility by producing a chimeric strain in which *Clgn*^{-/-} mice were crossed with a transgenic mouse in which the sperm acrosome was tagged using enhanced green fluorescent protein (GFP; Nakanishi et al., 1999). When these chimeras were mated with females, only the WT spermatozoa migrated into the oviduct, whereas the concomitantly ejaculated *Clgn*^{-/-} spermatozoa remained in the uterus (Nakanishi et al., 2004). From these results, it appears that correct interaction with the UTJ plays an important role in the migration of spermatozoa into the oviducts.

A disintegrin and metallopeptidase domain 3 (ADAM3) requires assistance from at least seven other genes to be delivered properly onto the sperm surface, and in all of the reported gene-disrupted mouse lines indicated earlier (except for *Ace*, in which the microlocalization of ADAM3 on spermatozoa is impaired), ADAM3 is always missing from the sperm membrane (Ikawa et al., 2010; Tokuihiro et al., 2012). Thus the lack of ADAM3 on the sperm surface could be the major reason for the infertility of these gene-disrupted mouse lines. However, there is no concrete evidence that ADAM3 is the element that is ultimately responsible for sperm migration through the UTJ. To examine whether elements other than ADAM3 might be responsible for sperm–UTJ interaction, we performed two-dimensional (2D) gel analyses on sperm extracts and found that there were two proteins missing in the spermatozoa from *Clgn*-disrupted mice. In the present article, we describe the identification of these proteins, which we named Protein Missing in Infertile Sperm 1 and 2 (PMIS1 and PMIS2, respectively). After cloning of the genes for these proteins (*Pmis1* and *Pmis2*), we produced two gene-KO mouse lines. *Pmis1*-deficient males showed no apparent phenotype, but *Pmis2* disruption resulted in male infertility with a similar phenotype as in the *Clgn*^{-/-} mouse line. Thus PMIS2 could be the factor responsible for normal sperm migration through the UTJ.

RESULTS

Search for proteins missing in *Clgn*-KO mouse spermatozoa

To examine whether there might be a factor other than ADAM3 that regulates the ability of spermatozoa to pass through the UTJ into the oviducts, we compared protein extracts from *Clgn*-KO mice spermatozoa with WT spermatozoa on 2D gels. Assuming that the responsible factor is a membrane protein, we analyzed the detergent-enriched fraction after the extraction of proteins using Triton X-114 and subsequent phase separation. The 2D gel patterns were almost the same in *Clgn*^{-/-} and WT spermatozoa as seen by silver staining. However, we found two spots that disappeared in *Clgn*^{-/-} spermatozoa at a PI of 6.7, *M_r* 24 kDa, and a pl of 4.9, *M_r* 18 kDa (Figure 1A and Supplemental Figure S1A). We named these proteins PMIS1 and PMIS2, respectively. We also observed that PMIS2 was missing in spermatozoa from *Calr3*^{-/-} mice (Figure 1A, c and f).

These spots were isolated from WT spermatozoa after Sypro-Ruby staining. After digestion of the proteins with trypsin, the peptides were subjected to analysis by liquid chromatography–tandem mass spectrometry (LC-MS/MS). We identified peptide fragments derived from the testis-specific expressed sequence tag (EST) data (predicted gene 128 [Gm128; NM_001024841] and RIKEN cDNA 4930479M11 [NR_027848]). We searched the National Center for Biotechnology Information database using these EST data and estimated the full coding regions (Figure 1B and Supplemental Figure S2). Northern blot analysis with a probe to full-length cDNA revealed that both of these genes are expressed specifically in the

testis (Figure 1C and Supplemental Figure S1B). The estimated sizes of *Pmis1* and *Pmis2* mRNAs obtained by Northern blotting were 0.98 and 0.68 kb, respectively. Moreover, when we performed reverse transcription PCR (RT-PCR) analysis using mRNA prepared from testes of 1- to 5-wk-old mice, we detected the *Pmis2* mRNA only from mice of age 3 wk or older, suggesting that this gene is expressed in germ cells later than the spermatid stage of spermatogenesis (Figure 1D).

PMIS1 consists of 350 amino acids with a calculated PI of 8.17 and a molecular mass of 38 kDa. However, these values were significantly different from the results obtained by the 2D gel. The *Pmis1* gene has putative splicing sites, and the hypothetical isoform consists of 190 amino acids with a PI of 6.75 and 21-kDa molecular mass (Supplemental Figure S2). The size of the RNA obtained by Northern blot was 0.98 kb, and this matched the calculated size of the spliced isoform. We estimate that some modifications must have taken place to the putative spliced form of PMIS1 because the molecular mass calculated from the position of PMIS1 on the 2D gel was less than that calculated from the amino acid sequence but greater than the mass calculated after taking into account the putative splicing sites.

PMIS2 consists of 96 amino acids with two hydrophobic regions bearing a single *N*-glycosylation site. The pI value of this protein was around 5.0 on the 2D gel, and this matched the calculated value of 5.04 based on the amino acid sequence. The apparent molecular mass on the 2D gel (18 kDa) was slightly greater than that of the calculated value (11 kDa), indicating that PMIS2 is probably modified in some manner that might include glycosylation.

Generation of *Pmis1*- and *Pmis2*-deficient mice and assessment of fertility

To test the functions of PMIS1 and PMIS2 in sperm migration into the oviduct, we generated *Pmis1* and *Pmis2* gene-disrupted mouse lines by homologous recombination (Figure 2A and Supplemental Figure S3). *Pmis1*^{-/-} male mice showed natural mating behavior and vaginal plug formation. Wild-type eggs recovered from the oviducts of superovulated female mice mated with *Pmis1*^{-/-} males (*n* = 3) showed slightly lower fertilization rates than controls (*Pmis1*^{+/-}, 89.8 ± 10.9%; *Pmis1*^{-/-}, 61.7 ± 8.0%; *p* < 0.01); however, in natural mating conditions (*n* = 4), we found no difference in their litter sizes (*Pmis1*^{+/-}, 9.5 ± 2.4; *Pmis1*^{-/-}, 9.4 ± 2.3; *p* = 0.85; Supplemental Figure S4, A and B).

Concerning *Pmis2*, by mating heterozygous mice, we obtained the expected Mendelian ratios of pups (*Pmis2*^{+/+}, 31, or 28%; *Pmis2*^{+/-}, 58, or 52%; *Pmis2*^{-/-}, 23, or 20%; *n* = 112). We confirmed that the *Pmis2* mRNA was eliminated in the *Pmis2*^{-/-} testes (Figure 2C), and the PMIS2 protein was also undetectable in the testes and spermatozoa by Western blotting (Figure 2D). To examine the effect of *Pmis2*^{-/-} on fertilization, we placed the *Pmis2*-disrupted mice with WT mice for 3 mo. Pups were obtained from *Pmis2*^{+/-} males and *Pmis2*^{-/-} females, whereas *Pmis2*^{-/-} male mice sired no pups in spite of their normal mating behavior (Figure 3A). To investigate the cause of this male infertility more precisely, we mated *Pmis2*^{+/-} or *Pmis2*^{-/-} male mice with superovulated WT females. Eggs were collected from the oviducts after examining for the formation of a vaginal plug, and the fertilization rate was examined. We could obtain no fertilized eggs from the females that mated with *Pmis2*^{-/-} males, whereas almost 100% of the eggs were fertilized in the females mated with *Pmis2*^{+/-} males (Figure 3B). These results suggest that PMIS2 is essential for fertilization by natural mating.

Gene-KO experiments occasionally reveal phenotypes derived from unexpected side effects of the gene manipulation, such as

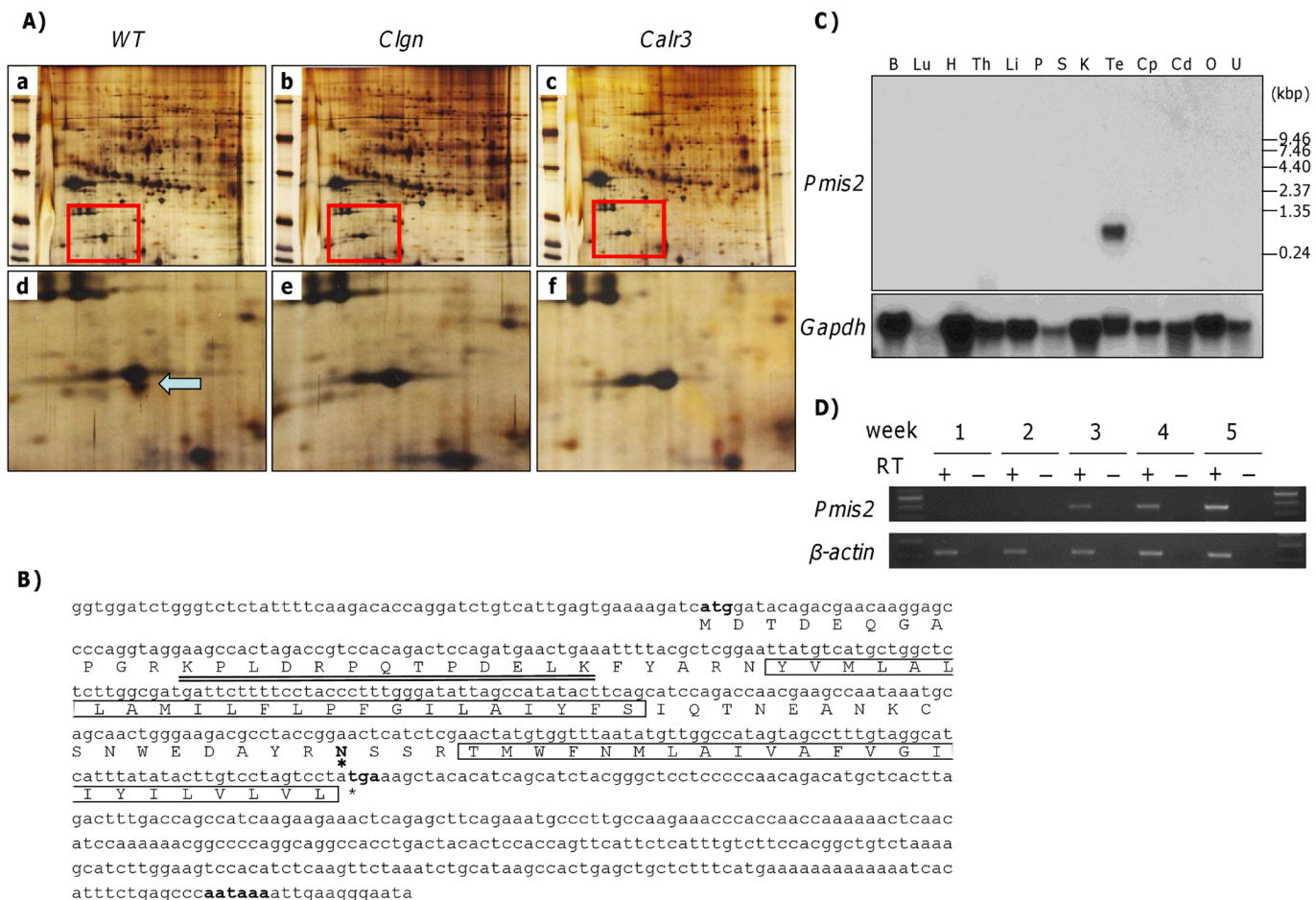


FIGURE 1: Identification of the testis-specific expressed gene *Pmis2*. (A) Comparison of sperm proteins separated on 2D gels among wild-type (WT) (a), *Clgn*^{-/-} (b), and *Calr3*^{-/-} (c) strains. (d-f) Enlargements of the boxes in a-c, respectively. The arrow represents the spot (PMIS2) missing in *Clgn*^{-/-} and *Calr3*^{-/-} spermatozoa. (B) DNA and amino acid sequence of *Pmis2*. The double underline is the peptide matched in the Mascot database. Boxed sequences indicate hydrophobic regions, and the asterisk indicates a putative N-glycosylation site. (C) Northern blot analysis revealed testis-specific expression of *Pmis2*. *Pmis2* cDNA was hybridized with total tissue RNA. Bottom, hybridization with *Gapdh* cDNA as control. B, brain; Cd, cauda epididymidis; Cp, caput epididymidis; H, heart; K, kidney; Li, liver; Lu, lung; O, ovary; P, pancreas; S, spleen; Te, testis; Th, thymus; U, uterus. (D) Time course of *Pmis2* expression in the testis. The expression of *Pmis2* becomes evident from 3 wk of age. Bottom, amplification of β -actin mRNA as control.

silencing a neighboring gene (Yoon et al., 1997) or exon jumping to an adjacent gene (Rossi et al., 2001). Therefore we generated transgenic mouse lines harboring hexahistidine (His6)-tagged *Pmis2* cDNA under the regulation of the *Clgn* promoter and performed a gene rescue experiment (Figure 3C). Although the protein was not recognized by anti-PMIS2 antibody, the expression of recombinant PMIS2 protein was detected using an anti-His antibody. Both of these transgenic mouse lines expressing His6-tagged PMIS2 protein were shown to rescue the infertile phenotype by being incorporated into the *Pmis2*^{-/-} genetic background (Figure 3, D-F), indicating that the recombinant PMIS2 with His6 tag could function normally and that infertility in the *Pmis2*^{-/-} mice was caused directly by the absence of PMIS2 from spermatozoa.

In the next experiment, we examined the fertilizing ability of spermatozoa from *Pmis2*^{-/-} males in vitro. These spermatozoa exhibited normal fusing ability when added to zona-free eggs (unpublished data). However, when the spermatozoa were mixed with zona-intact eggs, the zona-binding ability was significantly decreased compared with WT spermatozoa (Figure 4A). This phenotype was similar to those of spermatozoa lacking ADAM3. However,

as reported previously (Nishimura et al., 2004) for an *Adam1a*-disrupted mouse line, the loss of zona-binding ability did not result in the failure of in vitro fertilization (IVF) when cumulus-intact eggs were used (Figure 4B).

Impaired migration through the UTJ by PMIS2-deficient spermatozoa

Because the *Pmis2*^{-/-} spermatozoa were assumed to have a defect in oviduct migration, we crossed *Pmis2*^{-/-} mice with *Acr-EGFP*^{+/+} transgenic mice and examined the ability of their spermatozoa to penetrate the UTJ. This enabled us to visualize the migration of spermatozoa into the oviduct using a live-imaging system. A normal amount of spermatozoa was found in the uterus of females mated with GFP-tagged spermatozoa from *Pmis2*^{+/+} males together with many spermatozoa in the oviducts of these females (Figure 5, A-C). On the other hand, when the females were mated with *Pmis2*^{-/-} males producing GFP-tagged spermatozoa, no spermatozoa were found in the oviducts of female mice, whereas many spermatozoa were observed in the uteri (Figure 5, D-F). Thus *Pmis2*^{-/-} spermatozoa are unable to cross the UTJ.

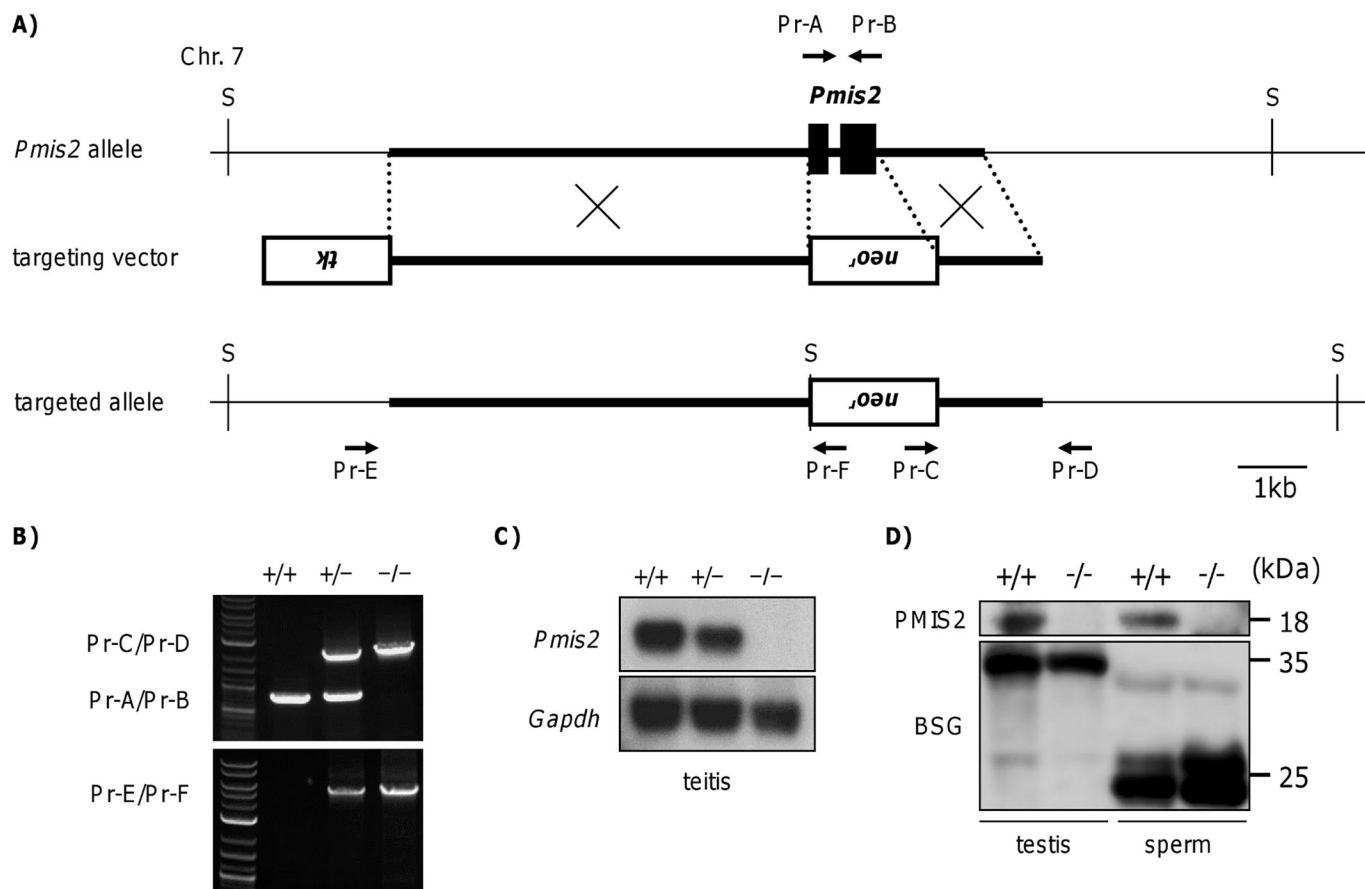


FIGURE 2: Generation of *Pmis2*-knockout mice. (A) A schematic diagram of the normal *Pmis2* allele and the targeted allele. The mouse *Pmis2* gene is located on chromosome 7 and is composed of two exons. Because *Pmis2* mRNA is expressed in the testis specifically, we constructed a targeting vector that replaced both of the exons with a neomycin-resistance gene. (B) Confirmation of homologous recombination using PCR. Top and bottom, the recombination of short and long arms, respectively. (C, D) Northern and Western blot analyses revealed the disappearance of *Pmis2* mRNA and PMIS2 protein in homozygous testes and spermatozoa. *Gapdh* mRNA and BASIGIN (BSG) protein, which expressed in testis and localized on sperm surface, were analyzed as control.

Fertilization-related proteins in PMIS2-deficient spermatozoa

To clarify the molecular nature of infertility observed in *Pmis2*^{-/-} males, we examined the fertilization-related proteins ADAM1a, ADAM2, ADAM3, testicular ACE (tACE), CLGN, and CALR3 in testes and spermatozoa. The last two are testis-specific molecular chaperones and act to fold ADAM family proteins. Both of these testis-specific chaperones remained unaffected in the *Pmis2*^{-/-} testis (Figure 6A). Although it is assumed that CLGN and CALR3 are involved in the folding of PMIS2, we were not able to detect the interaction of these chaperones with PMIS2 by immunoprecipitation studies.

The levels of CLGN, CALR3, ADAM1a, ADAM2, and ADAM3 were found to be normal in the testes of *Pmis2*^{-/-} males. The formation of ADAM1a/ADAM2 and ADAM1b/ADAM2 heterodimers was also found to be normal (Figure 6A). ADAM1b and ADAM2 expression levels also remained normal in the spermatozoa (Figure 6B). The expression of tACE was also found to be unaffected in *Pmis2*^{-/-} spermatozoa, indicating that PMIS2 must be the factor responsible for infertility. However, we were unable to verify this, as ADAM3 was absent in *Pmis2*^{-/-} spermatozoa. For a further analysis of the link between PMIS2 and ADAM3, we tested for the presence of the PMIS2 protein in *Adam3*^{-/-} spermatozoa. As shown in Figure 6C, PMIS2 became undetectable in spermatozoa after disruption of

Adam3. Thus PMIS2 and ADAM3 are both involved in sperm migration into the oviduct.

DISCUSSION

As a result of ongoing research into the mechanism of fertilization using gene-manipulated animals, a new scheme is emerging to replace the old models (Ikawa et al., 2010). Detailed analysis revealed that in at least seven gene-KO mouse lines (for *Clgn*, *Calr3*, *Pdilt*, *Tpst2*, *Ace*, *Adam1a*, and *Adam2*), ADAM3 became undetectable (or showed aberrant localization) in spermatozoa and the male mice were infertile (Cho et al., 1998; Nishimura et al., 2004; Yamaguchi et al., 2006; Ikawa et al., 2011; Marcello et al., 2011; Tokuyoshi et al., 2012). Therefore ADAM3 is considered to be a key molecule for ensuring fertility.

Even though they show vigorous movement, when they come into contact with zona pellucida WT spermatozoa stick to it very efficiently. All of the various kinds of ADAM3-deficient spermatozoa were shown to fail in binding to the zona pellucida of cumulus-free eggs. If we assume that ADAM3 is directly involved in sperm–zona binding, then quantifying ADAM3 on the sperm surface is of interest. The presence of ADAM3 on spermatozoa has been verified by Western blotting and immunostaining (Kim et al., 2004). However, as far as we know, ADAM3 has never been detected by a direct

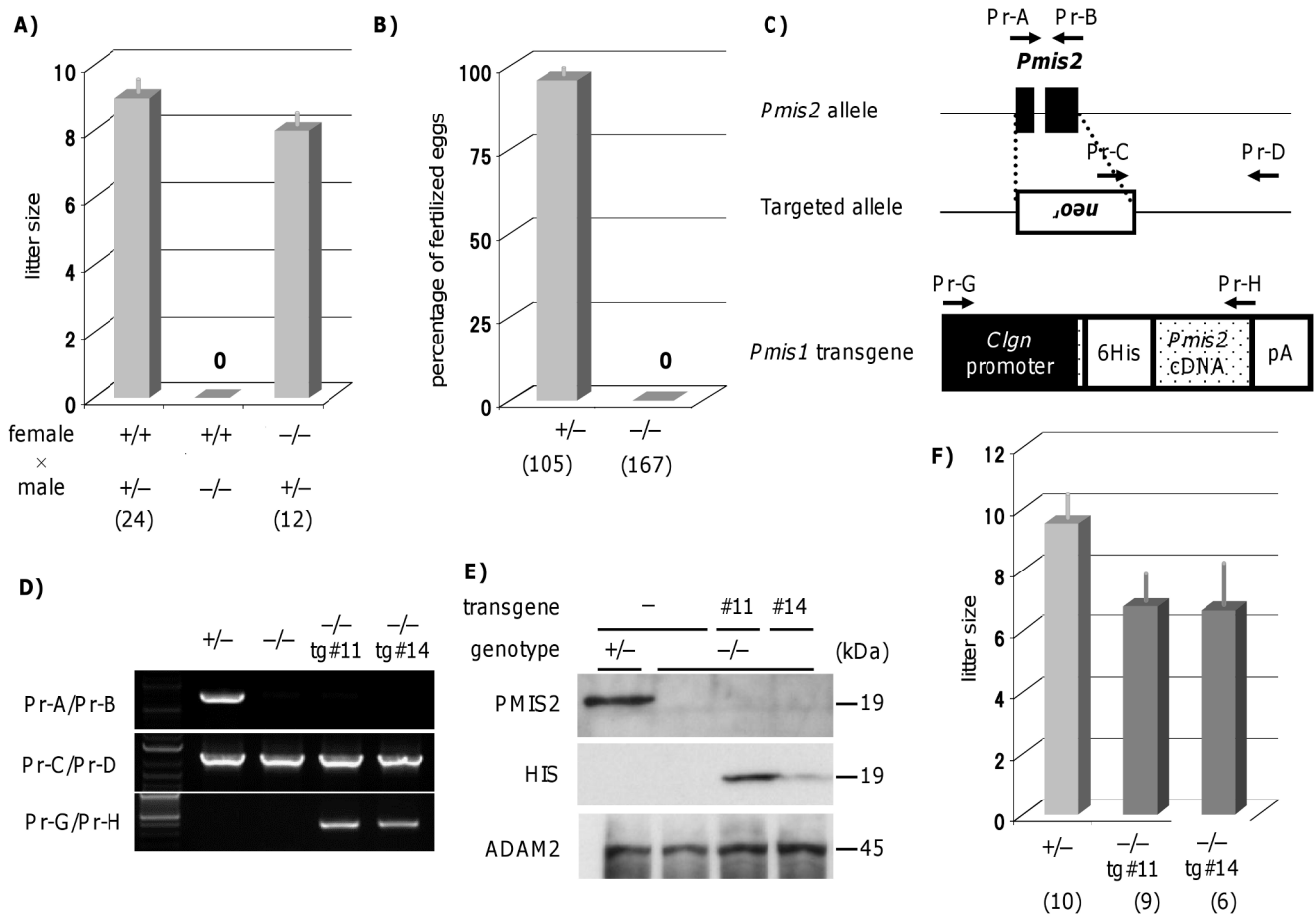


FIGURE 3: Defect of fertilization in *Pmis2*^{-/-} mice and transgenic rescue. (A) *Pmis2*^{+/-} males and *Pmis2*^{-/-} females delivered normal numbers of pups when mated with WT mice, whereas the combination of WT females with *Pmis2*^{-/-} males produced no pups. (B) The defect was at the fertilization level, because no fertilized eggs were recovered from the superovulated females mated with *Pmis2*^{-/-} males. Parentheses indicate the numbers of eggs examined. (C) Top, the targeting vector used to disrupt the mouse *Pmis2* allele. Bottom, the transgene used for rescue experiments to express *Pmis2* under the control of the *Clgn* promoter. The arrows indicate the positions of primer sets to detect the targeted alleles. (D) Genotyping of tail-tip DNA from various groups of mice by PCR amplification with the primers indicated in *Materials and Methods*. (E) Protein extracts from *Pmis2*^{+/-} and *Pmis2*^{-/-} and spermatozoa from transgenically rescued *Pmis2*^{-/-} mice were subjected to immunoblot analysis using anti-PMIS2 and anti-His-tag antibodies. ADAM2 was indicated as a reference marker for the successful extraction of proteins. (F) Litter sizes obtained by mating *Pmis2*^{+/-} and transgenically rescued *Pmis2*^{-/-} males with WT female mice. The sterile phenotype of *Pmis2*^{-/-} mice was restored by the insertion of the *Pmis2* transgene.

staining method on gels such as by silver staining or by proteomic analysis using mass spectrometry. We hypothesized that another molecule(s) might be more abundant than ADAM3 and function directly in sperm-egg binding. On the basis of this hypothesis, we performed a proteomic analysis of mouse sperm extracts and discovered the possible involvement of *Pmis1* and *Pmis2* in the fertilization process. Here we described the cloning of these genes and their disruption by homologous recombination. *Pmis1* was shown not to be essential for fertilization (Supplemental Figure S4), but *Pmis2* (RIKEN cDNA 4930479M11), registered as a noncoding gene, was found to be producing mRNA, and the PMIS2 protein was essential for fertilization.

Because PMIS2 became undetectable in sperm by disruption of *Clgn* or *Calr3*, we assumed that these chaperones are necessary to fold PMIS2 properly, but we could not demonstrate the interaction of PMIS2 with these molecules by immunoprecipitation. We also tried to identify the localization of PMIS2 on spermatozoa, but in

spite of multiple trials (e.g., the use of whole recombinant PMIS2 protein expressed in mammalian cells as an antigen), we were not able to obtain an antibody that worked for immunostaining of native PMIS2 or recombinant PMIS2 on spermatozoa. Therefore the interactions of PMIS2 with other molecules and the localization of PMIS2 on the spermatozoon need to be clarified to understand the function of PMIS2 in fertilization.

Spermatozoa from *Pmis2*-KO mice showed normal fertilizing ability in an IVF system with cumulus-enclosed eggs, despite their impaired zona-binding ability. We do not know why; however, this phenomenon was already reported in spermatozoa lacking ADAM3 (Nishimura et al., 2004; Tokuhiro et al., 2012). In spite of the normal fertilizing ability in IVF, *Pmis2*-disrupted males were infertile in natural mating. The spermatozoa from *Pmis2*^{-/-} mice had a deficiency in sperm migration into the oviduct. This indicates that the immediate cause of *Pmis2*^{-/-} male infertility is the inability of spermatozoa to reach the oviduct rather than impaired zona-binding ability.

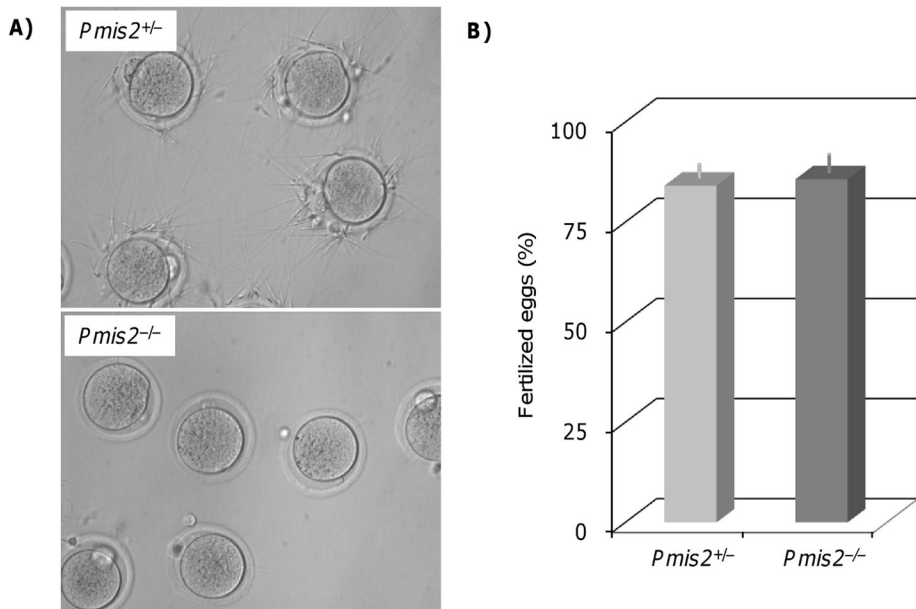


FIGURE 4: Assessment of the fertilizing ability of *Pmis2*^{-/-} spermatozoa by IVF. (A) *Pmis2*^{-/-} spermatozoa showed impaired zona-binding ability. (B) However, the spermatozoa were able to fertilize eggs, as well as WT spermatozoa, when added to cumulus-enclosed eggs.

Therefore the sperm–zona binding ability measured in vitro using cumulus-free eggs might not be a good indicator of the ultimate fertilizing ability of spermatozoa.

PMIS2 consists of two hydrophobic regions and a putative *N*-glycosylation site and shows homology to CD225 (also known as interferon-induced transmembrane protein 1) superfamily, based on motif searching. CD225 has been reported to mediate antiproliferative activity and cell–cell adhesion in human B cells and leukocytes (Deblandre *et al.*, 1995). If PMIS2 is related to the interaction of spermatozoa with the zona pellucida or with the epithelial cells of the UTJ, a common motif (amino acid sequence GAP to ILV) might be the responsible domain.

We found that PMIS2 was absent from spermatozoa in three independent mouse KO lines, for *Adam3*, *Clgn*, and *Calr3*. From its speculated abundance on spermatozoa, we assume that PMIS2 could be the ultimate factor involved in sperm migration into the oviduct, possibly based on an interaction of the sperm surface with the UTJ epithelium. However, when we disrupted *Pmis2*, ADAM3 became undetectable in the spermatozoa. Thus PMIS2 is the seventh gene discovered that is essential for ADAM3 to be delivered to the sperm surface. On the other hand, the disruption of *Pmis2* did not affect any of the remaining four gene products (CLGN, CALR3, ADAM1a, and ADAM2). Because both PMIS2 and ADAM3 become undetectable in spermatozoa if the other is not expressed, we assume that these proteins might interact closely. However, we have not been able to demonstrate the formation of heterodimers or direct interactions between the two proteins. The identification of PMIS2 as a novel candidate factor for the ultimate sperm–UTJ interaction (and also sperm–zona binding) will help clarify the general mechanism of mammalian fertilization.

MATERIALS AND METHODS

Two-dimensional gel electrophoresis

Cauda epididymal and vas deferens spermatozoa were collected in phosphate-buffered saline and resuspended in lysis buffer containing 1% Triton X-114. Sperm extracts were separated into two phases

as described (Yamaguchi *et al.*, 2006). Detergent-enriched fractions were resuspended in 8 M urea, 2% 3-[(3-cholamidopropyl)dimethylammonio]-1-propanesulfonate, and 10 mM dithiothreitol (DTT). After centrifugation, samples were desalted using MicroSpin G-25 columns (GE Healthcare UK, Little Chalfont, United Kingdom). Isoelectric focusing was performed in Immobiline DryStrip gels (pH 4–7) with IPG-phor (GE Healthcare UK) at 21°C, 50 μ A/strip, and 500 V (1 h), 1000 V (1 h), and 8000 V (4 h). Strips were equilibrated for 20 min in buffer containing 50 mM Tris/HCl (pH 6.8), 6 M urea, 30% glycerol, 1% SDS, and 25 mM DTT and then subjected to SDS–PAGE under reducing conditions. The gels were viewed after silver staining, and digital images were acquired by scanning. Unique spots were detected by visual judgment. Following SyproRuby staining, the spots were isolated and subjected to trypsin digestion. The resultant peptides were subjected to analysis by LC–MS/MS. The analysis was conducted in the APRO Life Science Institute (Tokushima, Japan). MS/MS spectra

were searched using the Mascot search engine (Matrix Science, Boston, MA).

Northern blot and RT-PCR analysis

Northern hybridization and RT-PCR were performed as described (Yamaguchi *et al.*, 2008; Fujihara *et al.*, 2010). Briefly, 10- μ g aliquots of total RNA extracted from various tissues of adult ICR strain mice (>2 mo old; Japan SLC, Shizuoka, Japan) were hybridized with the cDNAs for mouse *Pmis2* and glyceraldehyde-3-phosphate dehydrogenase (*Gapdh*). The *Pmis2* probe consisting of a cDNA fragment was amplified from mouse testis total RNA by PCR using 5'-GGAATTCGACACCAGGATCTGTCATTG-3' (Pr-A) and 5'-AGAATTCTGAAAGAGCAGCTCAGTGGC-3' (Pr-B) as primers.

These primers were used also for detection of the *Pmis2* WT allele.

For the *Gapdh* gene we used 5'-AGTGGAGATTGTTGCCATCAACGAC-3' and 5'-GGGAGTTGCTGTTGAAGTCGCAGGA-3'.

RT-PCR was performed using 10 ng of testicular cDNA from 1- to 5-wk-old ICR male mice using the forward and reverse primers 5'-AAGTGTGACGTTGACATCCG-3' and 5'-GATCCACATCTGCTGGAAGG-3', respectively, for the β -actin gene. Primers for *Pmis2* were the same as for the Northern blot analysis.

Generation of *Pmis2*-knockout mice

A targeting vector for the *Pmis2* gene disruption was constructed using the pPNT vector containing the Neo-resistance gene (*Neo*) as a positive selection marker and a herpes simplex virus thymidine kinase (*tk*) gene as a negative selection marker (Tybulewicz *et al.*, 1991). A 1.5-kb *NotI*–*XhoI* fragment as a short arm and a 6.0-kb *MfeI*–*KpnI* fragment as a long arm were obtained by PCR using genomic DNA of D3 embryonic stem (ES) cells as a template. The PCR primers used were 5'-AGCGGCCGCGGTAGGGAGTGCTTTAACCCACTAC-3' and 5'-TCTCGAGGTGTCTGGGTGTAGATGTTTCTCTGG-3' for the short arm and 5'-CCGGTACCGAGCTCCTTCAATGGCTGTAAGGACATCTC-3' and 5'-CCCAATTGACCAGAATCAGTCAGTCCAGG-3' for the long arm.

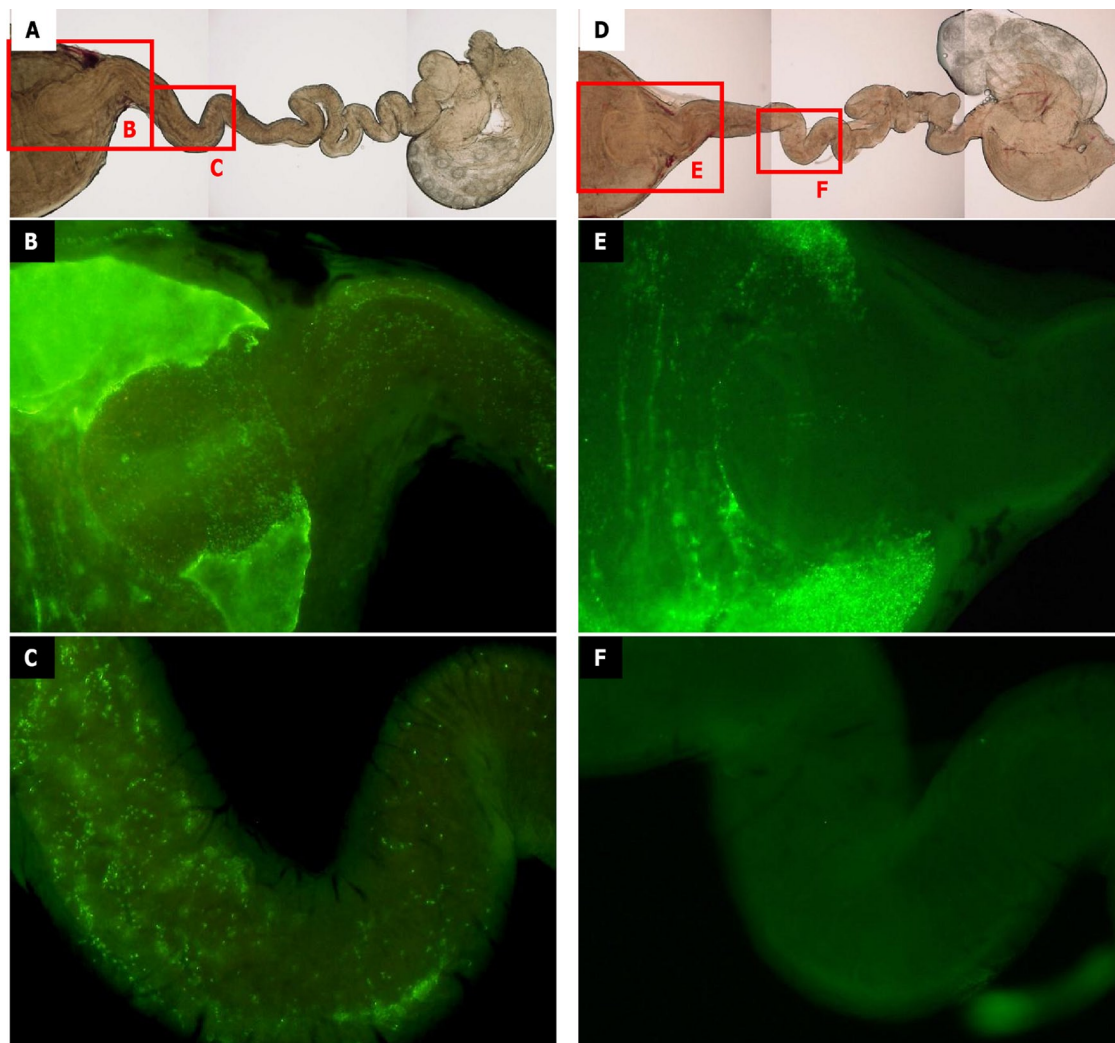


FIGURE 5: Impaired migration of *Pmis2*^{-/-} spermatozoa from the uterus to the oviduct. The migration of spermatozoa from the uterus to oviduct was examined 2 h after the observation of vaginal plugs in the females mated with males producing spermatozoa whose acrosome was tagged with enhanced GFP. (A–C) WT male mice. (D–F) *Pmis2*^{-/-} male mice. (F) There was no migration of *Pmis2*^{-/-} spermatozoa into the oviduct.

We detected the *Pmis2* mutant allele using the primer sets 5'-AGGGGAGGAGTAGAAGGTGGCGCAAGGGG-3' (Pr-C) and 5'-AGGATGGATTTCACAGGGCTAAGG-3' (Pr-D) for the short arm side and 5'-AGAGTACTGCTTGTGCTGCAGAGGG-3' (Pr-E) and 5'-CTTGACGAGT TCTTCTGAGG-3' (Pr-F) for the long arm side.

These two fragments were inserted into the pPNT vector, and the targeting construct was linearized using *NotI* digestion. ES cells were electroporated, and colonies were screened. The recombinant ES cell lines carrying the disrupted *Pmis2* allele were identified and subsequently used for generating chimeric embryos by injection into blastocysts from C57BL/6 Cr mice (>2 mo old; CLEA Japan, Tokyo, Japan). The injected blastocysts were transferred to pseudo-pregnant female mice (mated with vasectomized male mice), resulting in the birth of male chimeric mice. These mice were crossed with C57BL/6 female mice to obtain F1 generation heterozygous offspring. *PMIS2*-deficient mice were generated by the intercrossing of F1 offspring. The mice used in this study were of a B6;129 mixed background. All experiments on animals were performed with the approval of the Animal Care and Use Committee of Osaka University.

Production of *Pmis2* transgenic mice

His6-tagged mouse *Pmis2* cDNA with a rabbit polyA signal was inserted downstream of the *Clgn* promoter. The transgene cassette was injected into the pronuclei of zygotes from B6D2F1 mice (>2 mo old; CLEA Japan). Injected eggs were transferred to pseudo-pregnant females at the two-cell stage. Pups carrying the transgene were screened by PCR using the primers 5'-CCTTCCTGCGGCTT-GTTCTCT-3' (Pr-G) and 5'-CGAATTCTCATAGGACTAGGACAAG-3' (Pr-H).

IVF assay

Female B6D2F1 mice were superovulated after intraperitoneal injections of equine chorionic gonadotropin (eCG; Teikoku Zoki, Tokyo, Japan) and human chorionic gonadotropin (hCG; Teikoku Zoki) at 48-h intervals. Ovulated egg masses were recovered 13 h after the hCG injection and placed in a 200-μl drop of modified Krebs–Ringer bicarbonate solution (TYH medium; Toyoda et al., 1971) containing glucose, sodium pyruvate, bovine serum albumin, and antibiotics (0.05 mg/ml penicillin, 100 IU/ml streptomycin). Fresh spermatozoa from the cauda epididymidis were dispersed in

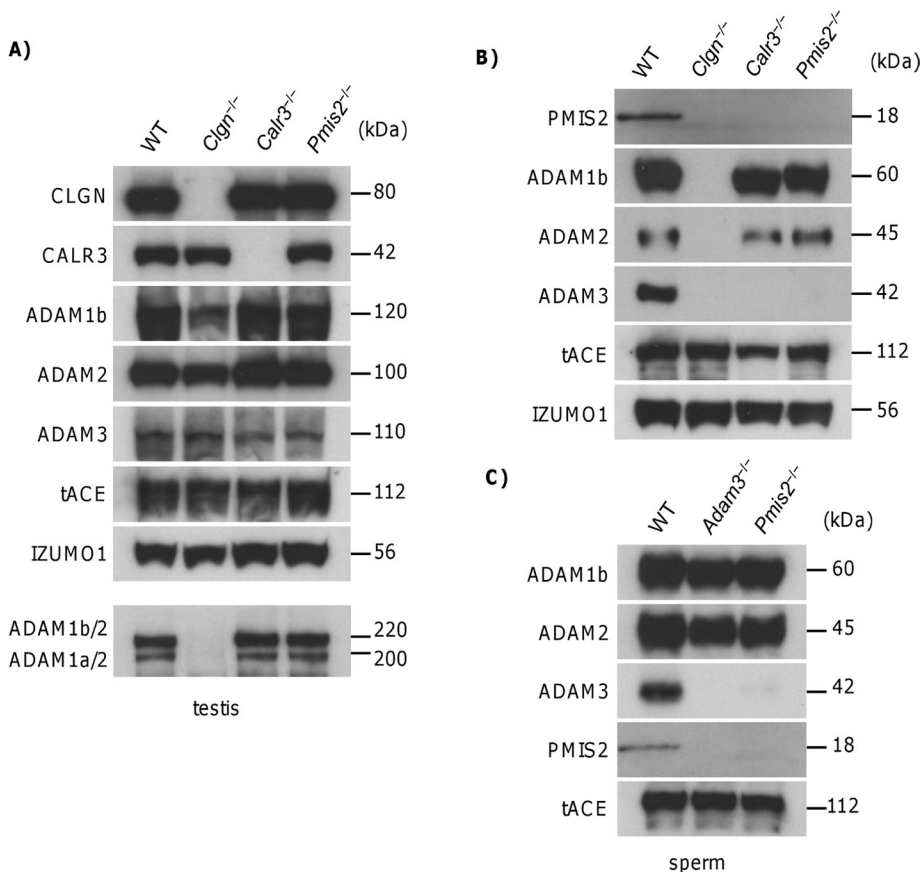


FIGURE 6: ADAM-family proteins in the various gene-disrupted male testes and spermatozoa. Protein extracts from *Clgn*^{-/-}, *Calr3*^{-/-}, and *Pmis2*^{-/-} testes (A) and spermatozoa (B) were separated by electrophoresis and subjected to immunoblot analysis. (A) Molecular chaperones and ADAM-family proteins were unaffected in *Pmis2*^{-/-} testes, including the normal formation of ADAM1/ADAM2 heterodimers. (B) PMIS2 disappeared in *Clgn*^{-/-} and *Calr3*^{-/-} spermatozoa, consistent with the result of 2D electrophoresis. ADAM1b and ADAM2 were found in *Pmis2*^{-/-} spermatozoa, but ADAM3—present in the testis—was not detected in spermatozoa. (C) Protein extracts from *Adam3*^{-/-} and *Pmis2*^{-/-} spermatozoa were subjected to immunoblot analysis. Both ADAM3 and PMIS2 proteins disappeared in spermatozoa from *Adam3*^{-/-} and *Pmis2*^{-/-} mice.

a 200- μ l drop of TYH medium, diluted to 1×10^6 spermatozoa/ml, and incubated for 1.5 h to induce capacitation. An aliquot of capacitated spermatozoa (2×10^5 spermatozoa/ml) from *Pmis2*-homozygous mutant males and heterozygous littermates was used for IVF. The mixture was incubated for 8 h at 37°C under 5% CO₂ in air. Fertilization was confirmed by pronuclear formation. For sperm-zona binding assays, egg masses were treated with bovine testicular hyaluronidase (175 U/ml; Sigma-Aldrich, St. Louis, MO) for 5 min to remove the cumulus cells. The cumulus-free eggs were placed in a 200- μ l droplet of TYH medium and inseminated as described. After 30 min of incubation, sperm binding to the zona pellucida of the eggs was observed using an IX-70 microscope (Olympus, Tokyo, Japan).

Fertility testing

Sexually mature male mice of the *Pmis2*^{+/-} and *Pmis2*^{-/-} genotypes were caged with B6D2F1 female mice for 3 mo, and the number of pups in each cage was counted within a week of birth. Female B6D2F1 mice were superovulated after intraperitoneal injections of eCG and hCG. *Pmis2*^{+/-} and *Pmis2*^{-/-} males were mated with superovulated females 7 h after hCG injection. Eggs were recovered from females at the pronuclear stage and cultured as described. Fertilization rates

were assessed by pronuclear formation and subsequent two-cell formation.

Sperm-UTJ transition assay

Females from a transgenic mouse line that expressed enhanced GFP in the acrosomes of spermatozoa (*Acr-EGFP*; Nakanishi et al., 1999) were crossed with *Pmis2*^{+/-} males. Double-transgenic F1 offspring were intercrossed to generate *Pmis2*^{-/-} and *Acr-Egfp*^{+/-} strains. These doubly transgenic mice were used for sperm migration analysis as described (Yamaguchi et al., 2009). Briefly, ~2 h after copulation, the uteri and oviducts were excised and straightened by cutting the mesosalpinx. They were transferred to slides and examined for the presence of spermatozoa expressing the acrosomal GFP marker, using a fluorescence microscope (BZ-8000; Keyence, Osaka, Japan). The experiments were performed twice, and we examined at least six different oviducts in each genotype. The number of mating pairs was five, using five different males. In each of two trials, three males made a vaginal plug. Thus we observed at least three and at most five different males.

Antibodies

A rabbit anti-mouse PMIS2 polyclonal antibody was produced by immunization of rabbits with the mouse PMIS2 peptide-KLH conjugate (CSNWEDAYRNSRTMWF-NML). Rat monoclonal antibodies (mAbs) against mouse IZUMO1 (MAB#125) and ADAM1b (MAB#158) were produced by immunization of rats with whole spermatozoa. Monoclonal antibodies against mouse ADAM2 (fertilin β ; 9D2.2) and ADAM3 (cyritestin; 7C1.2) were purchased from

Chemicon International (Temecula, CA). Rabbit polyclonal antibodies against CLGN and CALR3 and a mouse mAb against ACE were obtained as described (Yamaguchi et al., 2006; Ikawa et al., 2011).

Immunoblot analysis

Immunoblot analysis was performed as described (Ueda et al., 2007). Briefly, spermatozoa from the epididymis and vas deferens were collected and incubated in lysis buffer containing 1% Triton X-100 for 20 min on ice. The testes were excised, minced, and homogenized in lysis buffer and then placed on ice for 1 h. The spermatozoa and testis extracts were centrifuged, and the supernatants were collected. Proteins were separated by SDS-PAGE under reducing conditions and transferred electrophoretically to polyvinylidene fluoride membranes. After blocking, blots were incubated with primary antibodies overnight at 4°C and then incubated with horseradish peroxidase-conjugated secondary antibodies. The detection was performed using an ECL Western blotting detection kit (GE Healthcare UK). To detect ADAM1/2 heterodimers, testis extracts were separated by SDS-PAGE under nonreducing conditions at 4°C. Detection was performed using a mouse anti-ADAM2 mAb.

ACKNOWLEDGMENTS

We thank Y. Maruyama, A. Kawai, and Y. Koreeda for technical assistance in genetic manipulation. This work was supported in part by grants from the Ministry of Education, Science, Sports, Culture, and Technology of Japan and the 21st Century 200 Center of Excellence Program of the Ministry of Education, Culture, Sports, Science and Technology of Japan.

REFERENCES

- Cho C, Bunch DO, Faure JE, Goulding EH, Eddy EM, Primakoff P, Myles DG (1998). Fertilization defects in sperm from mice lacking fertilin beta. *Science* 281, 1857–1859.
- Deblandre GA, Marinx OP, Evans SS, Majaj S, Leo O, Caput D, Huez GA, Wathelet MG (1995). Expression cloning of an interferon-inducible 17-kDa membrane protein implicated in the control of cell growth. *J Biol Chem* 270, 23860–23866.
- Fujihara Y, Murakami M, Inoue N, Satouh Y, Kaseda K, Ikawa M, Okabe M (2010). Sperm equatorial segment protein 1, SPESP1, is required for fully fertile sperm in mouse. *J Cell Sci* 123, 1531–1536.
- Ikawa M, Inoue N, Benham AM, Okabe M (2010). Fertilization: a sperm's journey to and interaction with the oocyte. *J Clin Invest* 120, 984–994.
- Ikawa M, Tokuhiko K, Yamaguchi R, Benham AM, Tamura T, Wada I, Satouh Y, Inoue N, Okabe M (2011). Calsperin is a testis-specific chaperone required for sperm fertility. *J Biol Chem* 286, 5639–5646.
- Ikawa M, Wada I, Kominami K, Watanabe D, Toshimori K, Nishimune Y, Okabe M (1997). The putative chaperone calmeglin is required for sperm fertility. *Nature* 387, 607–611.
- Kim E, Nishimura H, Iwase S, Yamagata K, Kashiwabara S, Baba T (2004). Synthesis, processing, and subcellular localization of mouse ADAM3 during spermatogenesis and epididymal sperm transport. *J Reprod Dev* 50, 571–578.
- Krege JH, John SW, Langenbach LL, Hodgins JB, Hagaman JR, Bachman ES, Jennette JC, O'Brien DA, Smithies O (1995). Male-female differences in fertility and blood pressure in ACE-deficient mice. *Nature* 375, 146–148.
- Marcello MR, Jia W, Leary JA, Moore KL, Evans JP (2011). Lack of tyrosyl-protein sulfotransferase-2 activity results in altered sperm-egg interactions and loss of ADAM3 and ADAM6 in epididymal sperm. *J Biol Chem* 286, 13060–13070.
- Nakanishi T, Ikawa M, Yamada S, Parvinen M, Baba T, Nishimune Y, Okabe M (1999). Real-time observation of acrosomal dispersal from mouse sperm using GFP as a marker protein. *FEBS Lett* 449, 277–283.
- Nakanishi T, Isotani A, Yamaguchi R, Ikawa M, Baba T, Suarez SS, Okabe M (2004). Selective passage through the uterotubal junction of sperm from a mixed population produced by chimeras of calmeglin-knockout and wild-type male mice. *Biol Reprod* 71, 959–965.
- Nishimura H, Kim E, Nakanishi T, Baba T (2004). Possible function of the ADAM1a/ADAM2 Fertilin complex in the appearance of ADAM3 on the sperm surface. *J Biol Chem* 279, 34957–34962.
- Rossi D, Cozzio A, Flechsig E, Klein MA, Rulicke T, Aguzzi A, Weissmann C (2001). Onset of ataxia and Purkinje cell loss in PrP null mice inversely correlated with Dpl level in brain. *EMBO J* 20, 694–702.
- Shamsadin R, Adham IM, Nayernia K, Heinlein UA, Oberwinkler H, Engel W (1999). Male mice deficient for germ-cell cyritestin are infertile. *Biol Reprod* 61, 1445–1451.
- Suarez SS (2008). Regulation of sperm storage and movement in the mammalian oviduct. *Int J Dev Biol* 52, 455–462.
- Tokuhiro K, Ikawa M, Benham AM, Okabe M (2012). Protein disulfide isomerase homolog PDILT is required for quality control of sperm membrane protein ADAM3 and male infertility. *Proc Natl Acad Sci USA* 109, 3850–3855.
- Toyoda Y, Yokoyama M, Hoshi T (1971). Studies on the fertilization of mouse egg in vitro. *Jpn J Anim Reprod* 16, 147–151.
- Tybulewicz VL, Crawford CE, Jackson PK, Bronson RT, Mulligan RC (1991). Neonatal lethality and lymphopenia in mice with a homozygous disruption of the c-abl proto-oncogene. *Cell* 65, 1153–1163.
- Ueda Y, Yamaguchi R, Ikawa M, Okabe M, Morii E, Maeda Y, Kinoshita T (2007). PGAP1 knock-out mice show otocephaly and male infertility. *J Biol Chem* 282, 30373–30380.
- Yamaguchi R, Muro Y, Isotani A, Tokuhiko K, Takumi K, Adham I, Ikawa M, Okabe M (2009). Disruption of ADAM3 impairs the migration of sperm into oviduct in mouse. *Biol Reprod* 81, 142–146.
- Yamaguchi R, Yamagata K, Hasuwa H, Inano E, Ikawa M, Okabe M (2008). Cd52, known as a major maturation-associated sperm membrane antigen secreted from the epididymis, is not required for fertilization in the mouse. *Genes Cells* 13, 851–861.
- Yamaguchi R, Yamagata K, Ikawa M, Moss SB, Okabe M (2006). Aberrant distribution of ADAM3 in sperm from both angiotensin-converting enzyme (Ace)- and calmeglin (Clgn)-deficient mice. *Biol Reprod* 75, 760–766.
- Yoon JK, Olson EN, Arnold HH, Wold BJ (1997). Different MRF4 knockout alleles differentially disrupt Myf-5 expression: cis-regulatory interactions at the MRF4/Myf-5 locus. *Dev Biol* 188, 349–362.
- Zamboni L (1972). Moghissi KS, Hafez ESE (1972). Fertilization in the mouse. *Biology of Mammalian Fertilization and Implantation*, Springfield, IL: Charles C Thomas, 213–262.